

Chapter 2

The Company Eta Carinae Keeps: Stellar and Interstellar Content of the Carina Nebula

Nolan R. Walborn

Abstract The remarkable, interrelated stellar and nebular constituents of η Carinae's habitat, the giant Carina Nebula (NGC 3372), are reviewed. They are relevant to the interpretation of η Car itself. They include some of the hottest and most massive O stars known, frequently in close multiple systems; mysterious nebular structures; recently recognized ongoing star formation; the most extreme high-velocity interstellar absorption-line profiles in the Galaxy; and both stellar and diffuse X-ray sources.

2.1 Introduction

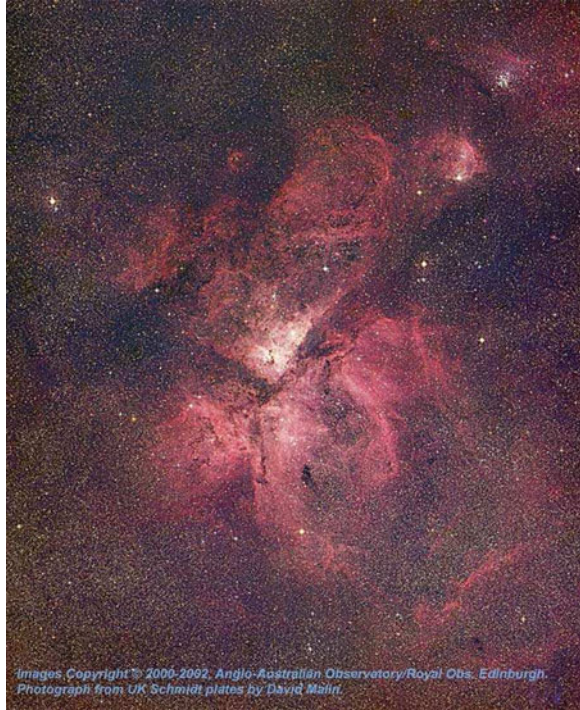
The fame and brilliance of η Carinae sometimes overwhelm its equally fascinating stellar and nebular environment. But the context of associated phenomena can provide vital clues to the nature of what may otherwise appear to be a bizarre peculiar object, for instance, its initial mass and age. In fact, the giant H II region known as the Carina Nebula, or NGC 3372, is one of the most powerful laboratories for investigation of the early evolution of the most massive stars, because of its relative proximity and moderate extinction, independently of η Car itself. The hottest spectral class, type O3, (now expanded to O2 through O3.5) was first recognized there. The massive stellar content of the Carina Nebula has been reviewed in detail by Walborn [77] and Smith [58]. Current star formation, likely triggered by the first-generation O stars, a ubiquitous characteristic of giant H II regions, has only recently been recognized in the Carina Nebula as a result of new infrared observations. This region also harbors extreme and in some respects unique

N.R. Walborn (✉)

Space Telescope Science Institute, 3700 San Martin Drive, Baltimore, MD 21218, USA

e-mail: walborn@stsci.edu

Fig. 2.1 The entire Carina Nebula (Image made from UK Schmidt plates by David Malin)



high-energy phenomena, revealed by the interstellar absorption lines and X-rays. The Carina Nebula is a dynamic, transitory cauldron of astrophysical interactions from which we have yet much to learn (Fig. 2.1).

The distance to the Carina Nebula was reviewed by Walborn [77] and by Davidson and Humphreys [19]. Using the luminosities of the O-type stars in the ionizing cluster Trumpler 16, Walborn estimated its distance as $D \approx 0.8^{(R-4)} \times 2,250 \text{ pc}$ with a small formal error, while Davidson and Humphreys adopted $2,300 \pm 200 \text{ pc}$ based upon photometric distances to Tr 16 plus the expansion of the η Car ejecta measured by Allen and Hillier [4] ($\sim 2,200 \text{ pc}$). The spectroscopic/photometric parallaxes of the OB stars are uncertain because of anomalous reddening laws that may vary from star to star, and which remain to be determined from future ultraviolet through infrared analyses of their energy distributions. Color-magnitude diagram distance determinations are also uncertain, because of superimposed subclusterings with a range of ages, and subluminous, zero-age OB main sequences at progressively lower masses with increasing age. Overluminous pre-main sequences at still lower masses also complicate the analysis of color-magnitude diagrams. Moreover, in this direction we are looking down a spiral arm, so there are numerous background, as well as a few foreground, objects in the field. Subsequently, Meaburn [38], Davidson et al. [18], and Smith [57] independently

derived distances of 2,300, 2,250, and 2,300 pc, respectively, from the motions of the ejected nebulosity. Systematic errors dominate, but the quoted uncertainties are in the range of ± 100 to ± 200 pc. The four nebular parallaxes agree remarkably well. These results imply that the typical ratio of total to selective extinction must be $R \sim 4$ toward the ionizing stars [77]. *The distance of η Carinae, and by implication of the Carina Nebula with which it has been shown to be associated, is thus now well established at 2,300 pc.* The diameter of the H II region is about 40 pc, and the total mass of ionized hydrogen is of order $10^4 M_{\odot}$, a thousand times that of the Orion Nebula, but one to two orders of magnitude below that of 30 Doradus in the Large Magellanic Cloud.

2.2 Stellar Content

The principal ionizing clusters of the Carina Nebula are Trumpler 16 (Tr 16), which contains η Car, and the very compact Trumpler 14 (Tr 14) in the northern part (Fig. 2.2); and Collinder 228 (Cr 228) in the southern part of the Nebula. The O3 subclass was introduced by Walborn [73, 74] to describe six stars in Tr 14 and Tr 16 with spectral types earlier than the earliest (O4) MK standards. One of them, HD 93129A, the brightest star in Tr 14, presented a qualitatively new kind of O-type spectrum, with a narrow N IV $\lambda 4058$ emission line stronger than the normal Of N III $\lambda\lambda 4634\text{--}4640\text{--}4642$ lines, which was denoted as Of*, and strong N V $\lambda\lambda 4604\text{--}4620$ absorption lines. These N IV and N V features are present in O4f spectra, but much more weakly and with the N IV weaker than N III; that is, the O3f* spectrum is a higher-ionization analogue of the O4f. There are also three WN-A, or WNL (i.e., narrow-line, late-type, high-luminosity WN), stars present, which bear strong spectroscopic relationships to the O3f*, in terms of progressive envelope or wind development ([75, 81]; Fig. 2.3). One of the WN-A stars is in Tr 16, while the other two are at the western and southern edges of the Nebula. This stellar population corresponds to an evolutionary age of ≤ 2 Myr (recently reduced to that value by the recognition that this kind of WN star is likely still burning H in the core) and upper masses of $\geq 100 M_{\odot}$. Evidence that Tr 14 is somewhat younger (≤ 1 Myr), and Cr 228 somewhat older, was discussed by Walborn [77], as was the speculative possibility that the two errant WN-A stars are runaways from Tr 16. Because of the smooth spectroscopic progression from the associated types O3 V through O3 If* to WN-A, it is likely that η Car is a *post*-WN-A star, if its current state is essentially a product of very massive single-star evolution, as opposed to a binary interaction. Langer et al. [33] advocated the same progression from a theoretical standpoint, and Smith and Conti [60] from a rediscussion of WN spectra.

In a review of the O3 subclass [83], it was subdivided into 3 including the new types O2 and O3.5. HD 93129A is now the prototype of the O2 If* category on the basis of its large N IV/N III emission-line ratio (Fig. 2.4), while the other Carina

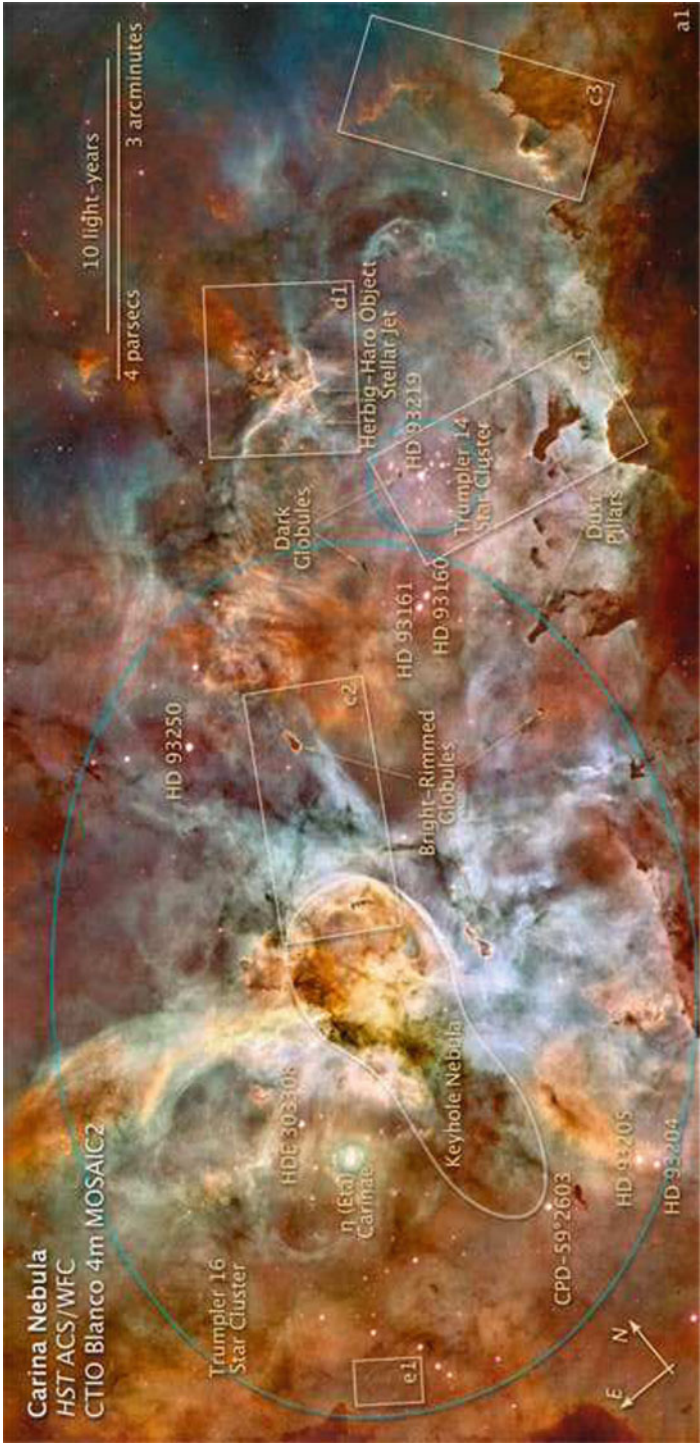


Fig. 2.2 The northern part of the Carina Nebula as imaged in H α by the advanced camera for surveys on the *Hubble Space Telescope*. Color has been added by means of groundbased images in other nebular lines from the Cerro Tololo Inter-American Observatory 4m telescope. The outlines and identifications of the principal features discussed in the text were added by Zolt Levay (STScI) (Image credit: NASA, ESA, Nathan Smith, and The Hubble Heritage Team (STScI/AURA))

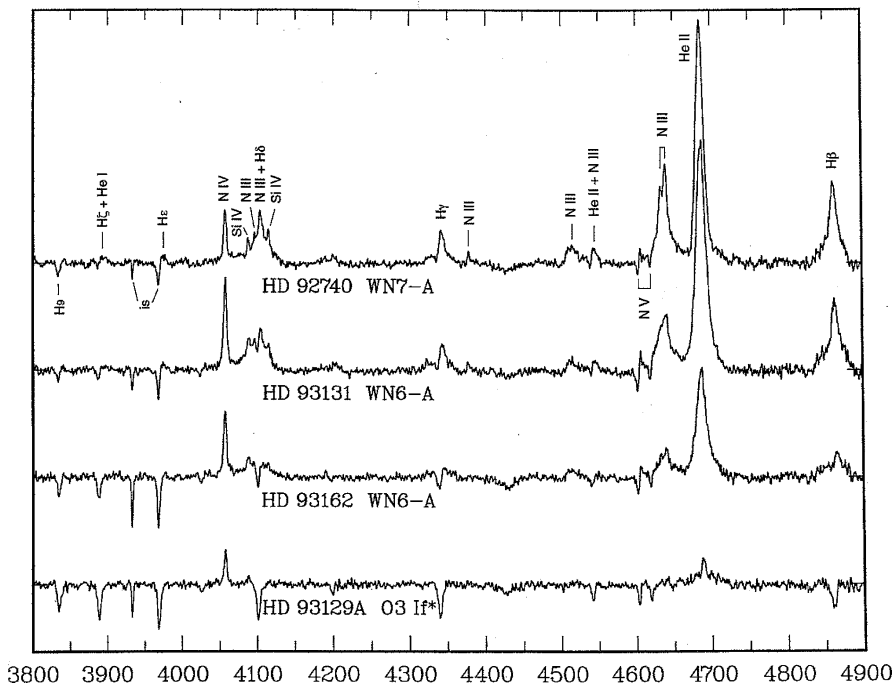


Fig. 2.3 Rectified, digital blue-violet spectrograms of HD 93129A (now O2 If*) and the three WN-A stars in the Carina Nebula (From [81])

Nebula members have been reclassified as O3.5 V((f+)), except one (HDE 303308) back to O4 V((f+)) based on the higher quality digital data now available (Fig. 2.5). (The ((f)) notation signifies strong He II $\lambda 4686$ *absorption* combined with weak N III emission; while the “+” qualifier denotes the additional presence of Si IV $\lambda\lambda 4089\text{--}4116$ emission lines, which is subsumed by f*.)

A large percentage of the most massive stars are found in spectroscopic binary and compact multiple systems; the Carina Nebula population is no exception. Outstanding examples are the O3.5 V((f)) + O8 V system HD 93205 [42] and the WN7-A + O8-9 HD 92740 [53]. Another interesting case is FO 15 (O5.5 Vz + O9.5 V; [45]; “Vz” means that the He II $\lambda 4686$ absorption line is stronger relative to other He lines than in normal class V spectra, indicating possible subluminality and zero-age-main-sequence status [80], which is supported by the physical parameters derived for this star. Triple lines have been found in the spectra of CPD $-59^\circ 2603$ (O7 V + O9.5 V + B0.2 IV; [50]) and CPD $-59^\circ 2636$ (O7 V + O8 V + O9 V; [1]). Even more extreme is the double spectroscopic binary HD 93206 in Cr 228 (O9.7 Ib:(n) + O9 III), which has two sets of lines with different periods [34, 43], but has yet to be resolved spatially despite attempts with groundbased speckle and the *HST* Fine Guidance Sensor interferometer.

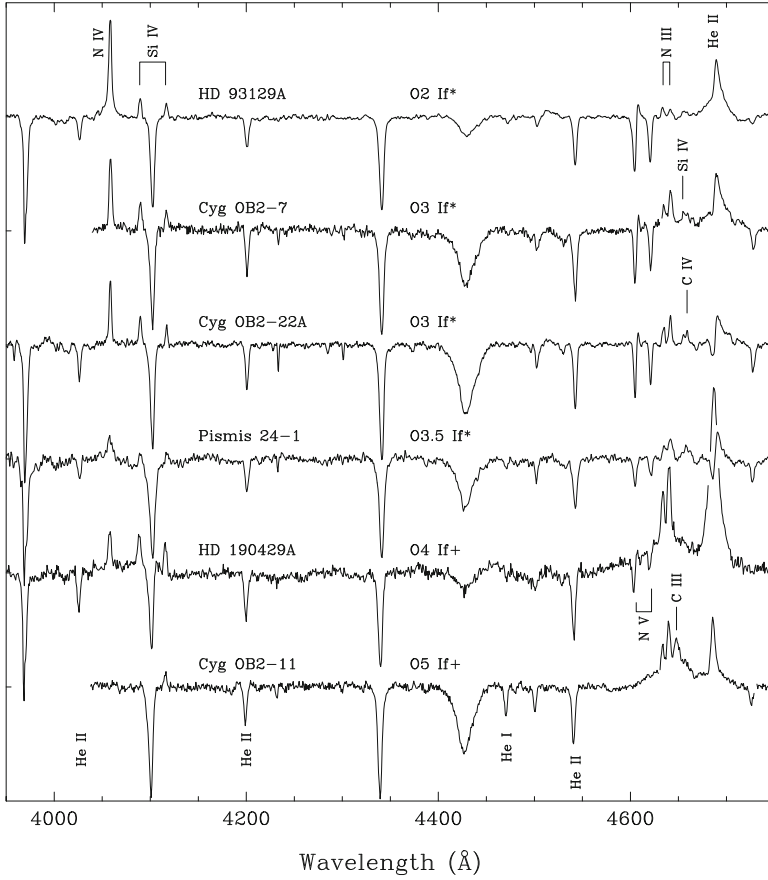


Fig. 2.4 An early Of supergiant spectral sequence, showing the extreme N IV/N III emission-line ratio in HD 93129A, leading to its earliest spectral type (Courtesy of Ian Howarth, from [79])

The Carina Nebula presents an attractive opportunity for a systematic investigation of multiplicity in an OB population, and such has been undertaken with *HST*/FGS [44]. Five new binaries were found in a preliminary subsample, including most remarkably HD 93129A with a separation of 55 milliarcsec and Δm_V of 0.9 (Fig. 2.6), likely implying yet another very early O main-sequence member of Tr 14. This pair was subsequently resolved in direct images with the *HST* Advanced Camera for Surveys (Fig. 2.7), and even more remarkably, relative motion of the components has been detected with both instruments; this is the most massive visual/astrometric binary known [36]. Likely related high-energy observations of the system are discussed later. HD 93129A (now Aab) has provided an anchor point for both the classification and quantitative analysis of the most massive stars (e.g., [70]). These results for relatively nearby stars emphasize anew the fundamental issues introduced by the endemic multiplicity of the O stars, frequently at

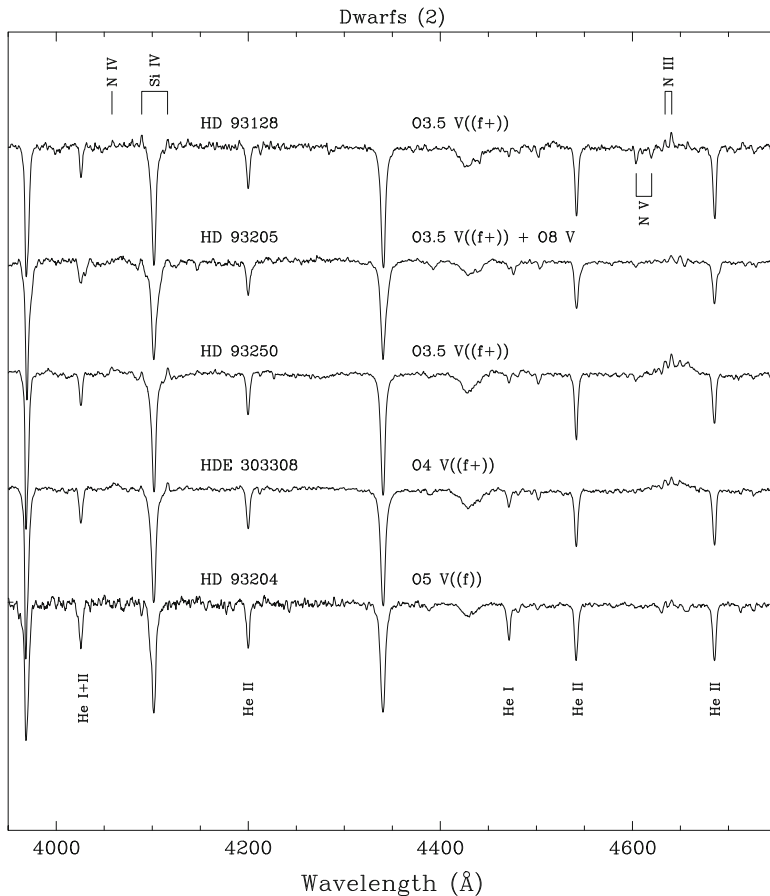


Fig. 2.5 An early O dwarf spectral sequence in the Carina Nebula (From [83])

or beyond the detection capabilities of current techniques, and the importance of continually addressing them at the state of the art. A binary nature of η Car would not be surprising, in view of the characteristics of its associated population.

Extensive spectroscopic, optical and/or infrared photometric, and astrometric studies of the Carina Nebula clusters [6, 20, 37, 68, 72] have provided useful data and interesting discussions. Nevertheless, the large disparities in reddening, distance, and age results document the uncertainties summarized in the Introduction above. It is likely that they will remain unresolved until UV–IR energy distributions and space interferometric astrometry become available for hundreds of individual stars. Smith [58] has made a complete census of the known OB stellar content of the Carina Nebula and calculated their radiative and mechanical energy inputs to the Nebula, which are relevant to the following sections.

Fig. 2.6 *HST* Fine Guidance Sensor scan of HD 93129Aab and B, showing the duplicity of the former (From [44] (The broad dip between the two stellar traces is an artifact))

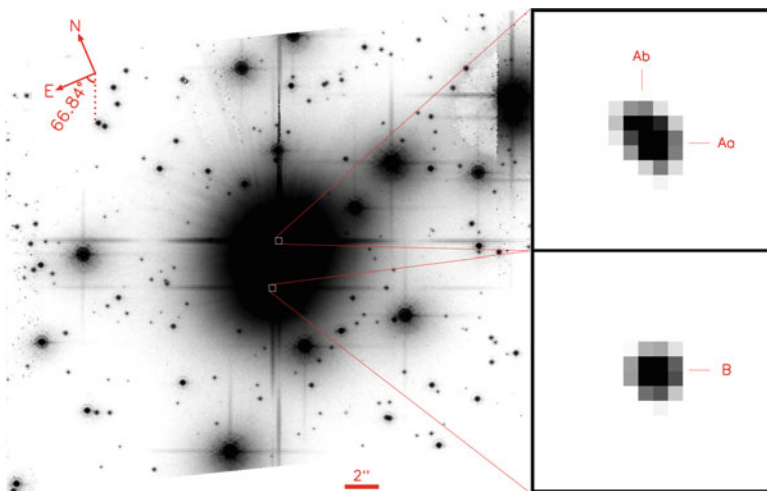
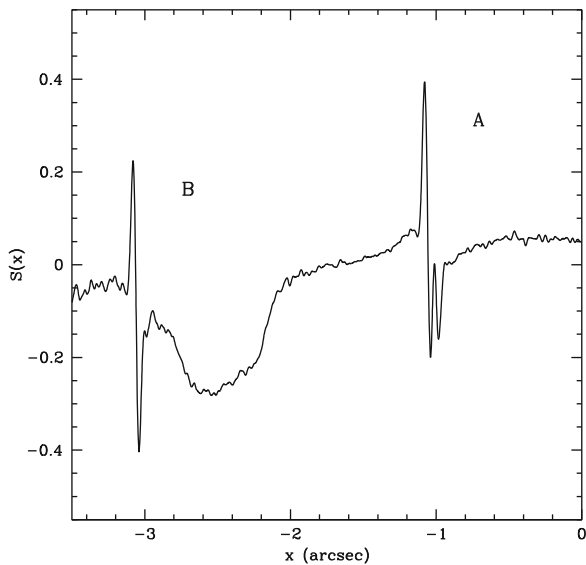


Fig. 2.7 *HST* Advanced Camera for Surveys High Resolution Camera images of the same two stars. (*left*) F850LP image of the HD 93129 system. (*right*) Enlargements of Aab (*top*) and B (*bottom*) from the F220W image. The separation of the former pair measured from this image is 51 milliarcsec in the N-S direction. An HRC pixel is $0.025''$ square and each of the right panels is $0.4''$ square (Courtesy of Jesús Maíz Apellániz)

2.3 Nebular Structures

The early radio-continuum observations of the Carina Nebula revealed two strong peaks in the northern part of the nebula, called Carina I and II [27]. They coincide with optical structures, the first with a semicircular dust incursion into the H II near the compact cluster Tr 14 (Fig. 2.2), lower corner of “c1” box, and the second with a curious apparent bright ring a few arcminutes northwest of η Car (Fig. 2.2, top of “Keyhole Nebula”, further discussed below). Subsequent radio observations with higher spatial resolution showed greater complexity in these structures [12, 31, 51, 86].

Deharveng and Maucherat [21] and Walborn [76] showed that the Car II ring is a physical structure best defined in the light of [S II]. There are other strange [S II] structures in the vicinity, and the general appearance of the northern part of the Carina Nebula is completely different in the light of [O III]. The gas kinematics of the region was further investigated by Meaburn et al. [39], and Kennicutt et al. [32] have discussed the implications of this inhomogeneity for standard nebular analyses, finding that the oxygen abundance is unaffected but there are problems with nitrogen and sulfur. Images of the Car II ring with the *HST* Wide Field Planetary Camera 2 revealed further intricate details, including barely resolved dark globules and the astounding adjacent “Finger Nebula”, evidently sculpted by the WN star HD 93162 (Fig. 2.8; [78]). The ring may have been created by η Car’s polar wind [56], and the apparently helical structure at its western edge might be a “twisted trunk” [15]. The Finger Nebula was analyzed in detail by Smith et al. [65] and is further mentioned below in the context of ongoing, triggered star formation. Smith et al. [67] also



Fig. 2.8 *HST* Wide Field Planetary Camera 2 image of the Keyhole/Carina II ring and the Finger Nebula (Credit: NASA, ESA, the author, Rodolfo Barbá, and The Hubble Heritage Team)

discussed further aspects of the possible interactions of η Car’s winds with the immediately surrounding region of the Nebula.

The association of η Car with the Carina Nebula has been demonstrated twice, first by Walborn and Liller [82] who discovered nearby dust clouds reflecting the peculiar spectrum of the star, and then by Allen [3] who showed that the redward component of the double nebular emission lines is occulted by the Homunculus. López and Meaburn [35] found that the reflected $H\alpha$ profile is different from that observed directly toward η Car and suggested a lagged time variation; however, [10, 62] reinterpreted the difference as caused by the spatial anisotropy of the wind emission, with the reflection revealing the polar profile. The presence of reflection has important implications for the drawing of the Carina Nebula by John Herschel at the time of η Car’s Great Eruption during the nineteenth century. He drew the bright nebulosity immediately to the west of the variable as far brighter and more extensive than it appears today, defining his “Keyhole Nebula” (the upper part of which is the Car II ring). The accuracy of Herschel’s drawing was questioned by Bok [9] on the assumption that the nebulosity was entirely ionized; η Car at maximum would not have been hot enough to excite it, and the recombination time would have been far longer in any event. Since we now know that this nebulosity has a reflection component, it is likely that the latter was considerably brighter when the variable was at maximum, and that it faded with a short lag during the subsequent decline, so that Herschel’s drawing is correct.

Molecular observations toward the Carina Nebula provide a different, complementary perspective. Early observations in the H_2CO and OH lines showed two strong peaks, coincident not with the radio-continuum maxima but with the dense V-shaped dust lanes that divide the northern and southern parts of the Nebula [22, 23, 28]. More extensive CO observations revealed an elongated giant molecular cloud with a mass of order $10^5 M_\odot$, the Carina Nebula being located near one end [29]. CO observations with higher spatial resolution discovered discrete cloudlets with masses of order $10 M_\odot$ in the vicinity of Car II [16], which are undoubtedly related to the subject of the following section. Infrared H_2 and PAH [11] and mm continuum [14] observations have been made in the same region; while far-IR line, CO, and CS have been observed throughout the Nebula [13, 41, 88].

Smith and Brooks [59] presented a thorough discussion of the global properties and energetics of the Carina Nebula, based on multiwavelength observations and a census of the inputs from the current stellar content. They conclude that the latter energy is more than sufficient to account for the IR luminosity, ionization, and kinematics of the Nebula, so there is no need to invoke an SNR in the region on energetic grounds.

2.4 Current Star Formation

Until recently, the Carina Nebula was generally regarded as an evolved H II region, with no particular evidence of ongoing star formation. However, more powerful IR (and optical) instrumentation in the Southern Hemisphere and in space has



Fig. 2.9 Enlargement from Fig. 2.2 of pillar and jet structures signaling new star formation in the northern Carina Nebula (Credit: NASA, ESA, Nathan Smith, and The Hubble Heritage Team)

drastically revised that perspective. Megeath et al. [40] discovered a small IR cluster within a bright-rimmed globule southeast of and facing η Car and Tr 16. A larger scale view from the *Midcourse Space Experiment* revealed a number of similarly oriented dust pillars and IR sources somewhat further to the southeast [61]. There are some additional cloudlets near Car II, as well as three possible ultracompact H II regions and a young stellar object with a disk in the vicinity of Tr 14 [48]. Numerous protoplanet candidates were found in groundbased images [63], and many more will undoubtedly be reported from the ACS images (Fig. 2.2). It is quite possible that the “Finger Nebula” noted above will give birth to a small cluster of low-mass stars, if the condensations responsible for its protuberances are sufficiently dense [65]. A giant Herbig-Haro flow was discovered in the southern part of the Nebula [64], and another small, newborn cluster nearby [30, 49, 66]. Several CO cores associated with IR sources and outflows, and further young objects in the vicinity of Tr 14 and Car I, have been presented [69, 87], respectively. The unprecedented pillar plus jet structures in Fig. 2.9, from the ACS data, appear to have been generated by the O6 stars HD 93160 and HD 93161AB (Fig. 2.2); they will enlighten us further about the physics of triggered star formation not only in Carina, but in general. Thus, the Carina Nebula also displays the ubiquitous evidence for triggered, second-generation star formation in H II regions [78]. Even more spectacular massive star formation will likely be triggered soon around the periphery of the current stellar-wind bubble in the Nebula, when η Car and its massive siblings end their lives as core-collapse supernovae [59].

2.5 Interstellar Absorption Lines

The interstellar absorption lines toward stars in the Carina Nebula have been studied by the author and collaborators for many years with progressively more powerful instrumentation, up to the state of the art with the *HST* Space Telescope Imaging Spectrograph ([17, 84, 85]; and references therein; Fig. 2.10). They present the most extreme profiles known in the Galaxy, similar in fact to some QSO narrow-line systems. Radial velocities in the strong, low-ionization lines range from nearly -400 to $+200 \text{ km s}^{-1}$, with up to 26 components resolved in a single line of sight. The rapid spatial variations in the profiles over small angular distances, higher frequency of complex profiles toward more massive stars, and large temporal variations in several components toward one star observed twice with STIS, all suggest that the high-velocity features arise in the near foregrounds of the stars toward which they are observed, i.e. within the Nebula. Although a model does not yet exist, interaction between the stellar winds and dense surrounding material is a possible origin of the phenomenon. Alternatively, Walborn et al. [85] emphasized the ubiquity of positive- as well as negative-velocity components, which may indicate expanding “shells” predominantly in the foreground of the stars, and thus possibly related to star-formation activity or an SNR on the near side of the Nebula. If this kinetic energy is being converted to thermal energy by collisions, temperatures of a few million degrees would result, which is likely relevant to the following section.

In contrast, the dominant components in the high-ionization and excited-state interstellar lines have velocities similar to the blueward components of the double nebular emission lines, that is, they arise in the near side of the globally expanding H II region. Thus, they provide valuable absorption diagnostics of the ionized material.

2.6 X-Rays

The *Einstein Observatory* discovered that all of the bright stars in the Carina Nebula, including η Car, are X-ray sources, but more surprisingly, that the entire Nebula is a source of diffuse soft X-rays [54, 55]. The more advanced capabilities of the *Chandra Observatory* and *XMM-Newton* have greatly expanded those early results [2, 5, 24, 25, 52, 71]. In particular, X-ray emission from tens of additional OB stars as well as hundreds of likely T Tauri stars has been found. The latter contributed to the original “diffuse” emission, but a true diffuse component remains. In view of the energy correspondence, the diffuse X-rays are very likely related to the high-velocity motions revealed by the interstellar absorption lines, as discussed in the previous section. An extensive new survey of the Carina Nebula undertaken by *Chandra* during 2007 (PI L. Townsley) will provide even more detailed information.

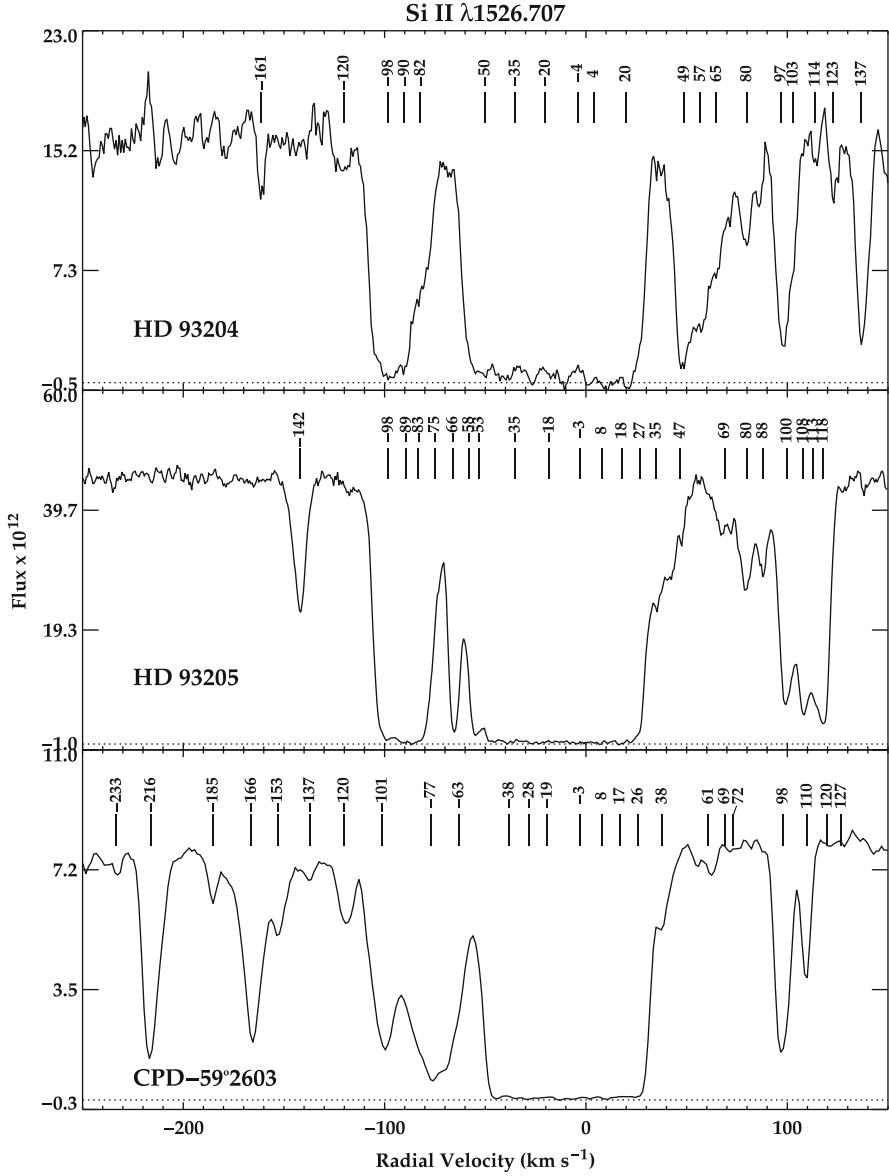


Fig. 2.10 Examples of extreme high-velocity interstellar absorption-line structure in the Carina Nebula. HD 93204 and HD 93205 are just $20''$ apart, or 0.22 pc in projection (From [85])

Several of the OB and WR members of the ionizing clusters have unusually hard X-ray spectra, indicating possible binary colliding-wind emission. Three of them are of outstanding interest and have related UV/optical/radio properties. One of them is HD 93129A, the O2 If* prototype and massive astrometric binary that dominates Tr 14, as discussed above. It has also been found to be a nonthermal radio source [7, 8]. Another is the WN6-A member of Tr 16 HD 93162, the sculptor of the “Finger Nebula”, which has one of the the highest X-ray luminosities known for a Wolf-Rayet star. It may be a colliding-wind binary on that basis [46, 47], and it has subsequently been found to be a long-period spectroscopic binary [26]. Finally, the remarkable X-ray and related properties of the likely binary η Car itself are discussed elsewhere in this volume. The primaries of these systems may well represent an evolutionary sequence of stars near the upper stellar mass limit.

2.7 Summary

Numerous studies have revealed the remarkable population of very massive stars and the complexity of the environment associated with η Car. But, as has been emphasized, we still need the multiwavelength spectral energy distributions of many of these stars to accurately determine their total luminosities and initial masses for comparison with η Car.

One of the outstanding problems in our present understanding of star formation, and of the Carina Nebula in particular, is why so many extremely massive stars form in such close proximity and at essentially the same time. What is the formation mechanism of such very massive stars?

References

1. J.F. Albacete Colombo, N.I. Morrell, G. Rauw, M.F. Corcoran, V.S. Niemela, H. Sana, Optical spectroscopy of X-Mega targets–IV. CPD -59° 2636: a new O-type multiple system in the Carina Nebula. *MNRAS*. **336**, 1099–1108 (2002)
2. J.F. Albacete Colombo, M. Méndez, N.I. Morrell, XMM-Newton X-ray observations of the Carina nebula. *MNRAS*. **346**, 704–718 (2003)
3. D.A. Allen, The location of Eta Carinae in NGC 3372. *MNRAS*. **189**, 1P–4P (1979)
4. D.A. Allen, D.J. Hillier, The shape of the Homunculus Nebula around Eta Carinae. *PASA*. **10**, 338–341 (1993)
5. I.I. Antokhin, G. Rauw, J.M. Vreux, K.A. van der Hucht, J.C. Brown, XMM-Newton X-ray study of early type stars in the Carina OB1 association. *A&A*. **477**, 593–609 (2008)
6. J. Ascenso, J. Alves, S. Vicente, Lago MTVT: NTT and VLT diffraction limited imaging of Trumpler 14: revealing a massive core-halo cluster. *A&A*. **476**, 199–215 (2007)
7. P. Benaglia, B. Koribalski, Radio observations of HD 93129A: the earliest O star with the highest mass loss? *A&A*. **416**, 171–178 (2004)
8. P. Benaglia, B. Koribalski, J.F. Albacete Colombo, Radio detection of colliding wind binaries. *PASA*. **23**, 50–63 (2006)

9. B. Bok, *A Study of the η Carinae Region*. Harvard Reprints Ser 1 No 77 (Harvard, Cambridge, MA, 1932), pp. 1–90
10. P. Boumis, J. Meaburn, M. Bryce, J.A. López, The H α echoes of η Carinae from 1985 to 1997. *MNRAS*. **294**, 61–68 (1998)
11. K.J. Brooks, M.G. Burton, J.M. Rathborne, M.C.B. Ashley, J.W.V. Storey, Unlocking the Keyhole: H $_2$ and PAH emission from molecular clumps in the Keyhole Nebula. *MNRAS*. **319**, 95–102 (2000)
12. K.J. Brooks, J.W.V. Storey, J.B. Whiteoak, H110 α recombination-line emission and 4.8 GHz continuum emission in the Carina nebula. *MNRAS*. **327**, 46–54 (2001)
13. K.J. Brooks, P. Cox, N. Schneider, J.W.V. Storey, A. Poglitsch, N. Geis, L. Bronfman, The Trumpler 14 photodissociation region in the Carina Nebula. *A&A*. **412**, 751–765 (2003)
14. K.J. Brooks, G. Garay, M. Nielbock, N. Smith, P. Cox, SIMBA observations of the Keyhole Nebula. *ApJ*. **634**, 436–441 (2005)
15. P. Carlqvist, G.F. Gahm, H. Kristen, Theory of twisted trunks. *A&A*. **403**, 399–412 (2003)
16. P. Cox, L. Bronfman, The molecular gas content of the Keyhole nebula. *A&A*. **299**, 583–590 (1995)
17. A.C. Danks, N.R. Walborn, G. Vieira, W.B. Landsman, J. Gales, B. García, Rapid temporal variations of interstellar absorption lines in the Carina Nebula. *ApJ*. **547**, L155–L159 (2001)
18. K. Davidson, N. Smith, T.R. Gull, K. Ishibashi, D.J. Hillier, The shape and orientation of the Homunculus Nebula based on spectroscopic velocities. *AJ*. **121**, 1569–1577 (2001)
19. K. Davidson, R.M. Humphreys, Eta Carinae and its environment. *ARA&A*. **35**, 1–32 (1997)
20. K. DeGioia-Eastwood, H. Throop, G. Walker, K.M. Cudworth, The star formation history of Trumpler 14 and Trumpler 16. *ApJ*. **549**, 578–589 (2001)
21. L. Deharveng, M. Maucherat, Optical study of the Carina Nebula. *A&A*. **41**, 27–36 (1975)
22. H.R. Dickel, Carina Nebula: a possible interpretation of the molecular observations. *A&A*. **31**, 11–16, (1974)
23. H.R. Dickel, J.V. Wall, The OH absorption against the Carina Nebula. *A&A*. **31**, 5–10 (1974)
24. N.R. Evans, F.D. Seward, M.I. Krauss, T. Isobe, J. Nichols, E.M. Schlegel, S.J. Wolk, Chandra observations of associates of η Carinae. I. Luminosities. *ApJ*. **589**, 509–525 (2003)
25. N.R. Evans, E.M. Schlegel, W.L. Waldron, F.D. Seward, M.I. Krauss, J. Nichols, S.J. Wolk, Chandra observations of associates of η Carinae. II. Spectra. *ApJ*. **612**, 1065–1080 (2004)
26. R. Gamén, E. Gosset, N. Morrell, V. Niemela, H. Sana, Y. Nazé, G. Rauw, R. Barbá, G. Solivella, The first orbital solution for the massive colliding-wind binary HD 93162 (=WR 25). *A&A*. **460**, 777–782 (2006)
27. F.F. Gardner, D.K. Milne, P.G. Mezger, T.L. Wilson, The Carina nebula at 6 cm. *A&A*. **7**, 349–358 (1970)
28. F.F. Gardner, H.R. Dickel, J.B. Whiteoak, The H $_2$ CO absorption against the Carina Nebula. *A&A*. **23**, 51–54 (1973)
29. D.A. Grabelsky, R.S. Cohen, L. Bronfman, P. Thaddeus, Molecular clouds in the Carina arm—The largest objects, associated regions of star formation, and the Carina arm in the galaxy. *ApJ*. **331**, 181–196 (1988)
30. G.F. Hägele, J.F. Albacete Colombo, R.H. Barbá, G.L. Bosch, G287.84–0.82: an infrared star cluster in the Carina nebula. *MNRAS*. **355**, 1237–1243 (2004)
31. W.K. Huchtmeier, G.A. Day, The Carina Nebula at 3.4 and 6 cm. *A&A*. **41**, 153–164 (1975)
32. R.C. Kennicutt Jr., F. Bresolin, H. French, P. Martin, An empirical test and calibration of H II region diagnostics. *ApJ*. **537**, 589–612 (2000)
33. N. Langer, W.R. Hamann, M. Lennon, F. Najarro, A.W.A. Pauldrach, J. Puls, Towards an understanding of very massive stars. A new evolutionary scenario relating O stars, LBVs, and Wolf-Rayet stars. *A&A*. **290**, 819–833 (1994)
34. K.C. Leung, A.F.J. Moffat, W. Seggewiss, The massive multiple system HD 93206 (QZ Carinae) in the great Carina Nebula. *ApJ*. **231**, 742–750 (1979)
35. J.A. López, J. Meaburn, The broad Balmer profiles from η Carinae scattered by dust over the Car II region. *RMxAA*. **13**, 27–32 (1986)

36. J. Maíz Apellániz, L. Úbeda, N.R. Walborn, E.P. Nelan, IMF biases and how to correct them, in *Resolved Stellar Populations*, ed. by D. Valls-Gavaud, M. Chávez. arXiv:astro-ph/0506283 (2005 in press)
37. P. Massey, J. Johnson, Massive stars near Eta Carinae—The stellar content of Tr 14 and Tr 16. *AJ*. **105**, 1225–1233 (1993)
38. J. Meaburn, An updated proper-motion/spectropolarimetric distance to η Carinae, in *Eta Carinae at the Millennium*, ed. by J.A. Morse, R.M. Humphreys, A. Damineli. ASP Conference Series, vol 179 (ASP, San Francisco, 1999), pp. 89–95
39. J. Meaburn, J.A. López, D. Keir, Insect-eye, Fabry-Perot observations of the large-scale motions within the Carina nebula (NGC 3372, RCW 53). *MNRAS*. **211**, 267–276 (1984)
40. S.T. Megeath, P. Cox, L. Bronfinan, P.R. Roelfsema, Evidence for ongoing star formation in the Carina nebula. *A&A*. **305**, 296–307 (1996)
41. M. Mizutani, T. Onaka, H. Shibai, Origin of diffuse C II 158 micron and Si II 35 micron emission in the Carina nebula. *A&A*. **423**, 579–592 (2004)
42. N.I. Morrell, et al., Optical spectroscopy of X-Mega targets—II. The massive double-lined O-type binary HD 93205. *MNRAS*. **326**, 85–94 (2001)
43. N.D. Morrison, P.S. Conti, Spectroscopic studies of O-type binaries. VI—The quadruple system QZ Carinae (HD 93206). *ApJ*. **239**, 212–219 (1980)
44. E.P. Nelan, N.R. Walborn, D.J. Wallace, A.F.J. Moffat, R.B. Makidon, D.R. Gies, N. Panagia, Resolving OB systems in the Carina nebula with the Hubble space telescope fine guidance sensor. *AJ*. **128**, 323–329 (2004)
45. V.S. Niemela, N.I. Morrell, E. Fernández Lajús, R. Barbá, J.F. Albacete Colombo, M. Orellana, Optical spectroscopy of X-Mega targets in the Carina nebula—VI. FO15: a new O-type double-lined eclipsing binary. *MNRAS*. **367**, 1450–1456 (2006)
46. A.M.T. Pollock, M.F. Corcoran, Evidence for colliding winds in WR 25 from XMM-Newton observations of X-ray variability. *A&A*. **445**, 1093–1097 (2006)
47. A.J.J. Raassen, K.A. van der Hucht, R. Mewe, I.I. Antokhin, G. Rauw, J.M. Vreux, W. Schmutz, M. Güdel, XMM-Newton high-resolution X-ray spectroscopy of the Wolf-Rayet object WR 25 in the Carina OB1 association. *A&A*. **402**, 653–666 (2003)
48. J.M. Rathborne, M.G. Burton, K.J. Brooks, M. Cohen, M.C.B. Ashley, J.W.V. Storey, Photodissociation regions and star formation in the Carina nebula. *MNRAS*. **331**, 85–97 (2002)
49. J.M. Rathborne, K.J. Brooks, M.G. Burton, M. Cohen, S. Bontemps, The giant pillars of the Carina Nebula. *A&A*. **418**, 563–576 (2004)
50. G. Rauw, H. Sana, I.I. Antokhin, N.I. Morrell, V.S. Niemela, J.F. Albacete Colombo, E. Gosset, J.M. Vreux, Optical spectroscopy of XMEGA targets in the Carina Nebula—III. The multiple system Tr 16-104 (=CPD -59° 2603). *MNRAS*. **326**, 1149–1160 (2001)
51. D.S. Retallack, Radio emission from Eta Carinae and the surrounding nebula. *MNRAS*. **204**, 669–674 (1983)
52. K. Sanchawala, W.P. Chen, H.T. Lee, Y.H. Chu, Y. Nakajima, M. Tamura, D. Baba, S. Sato, An X-ray and near-infrared study of young stars in the Carina nebula. *ApJ*. **656**, 462–473 (2007)
53. J. Schweickhardt, W. Schmutz, O. Stahl, Th. Szeifert, B. Wolf, Revised mass determination of the super massive Wolf-Rayet star WR 22. *A&A*. **347**, 127–136 (1999)
54. F.D. Seward, T. Chlebowski, X-ray emission from the Carina Nebula and the associated early stars. *ApJ*. **256**, 530–542 (1982)
55. F.D. Seward, W.R. Forman, R. Giacconi, R.E. Griffiths, F.R. Harnden Jr., C. Jones, J.P. Pye, X-rays from Eta Carinae and the surrounding nebula. *ApJ*. **234**, L55–L58 (1979)
56. N. Smith, Near-infrared and optical emission-line structure of the Keyhole Nebula in NGC 3372. *MNRAS*. **331**, 7–12 (2002a)
57. N. Smith, Dissecting the Homunculus nebula around Eta Carinae with spatially resolved near-infrared spectroscopy. *MNRAS*. **337**, 1252–1268 (2002b)
58. N. Smith, A census of the Carina Nebula—I. Cumulative energy input from massive stars. *MNRAS*. **367**, 763–772 (2006) [err **368**, 1983–1984]
59. N. Smith, K.J. Brooks, A census of the Carina Nebula—II. Energy budget and global properties of the nebula. *MNRAS*. **379**, 1279–1292 (2007)

60. N. Smith, P.S. Conti, On the role of the WNH phase in the evolution of very massive stars: enabling the LBV instability with feedback. *ApJ*. **679**, 1467–1477 (2008)
61. N. Smith, M.P. Egan, S. Carey, S.D. Price, J.A. Morse, P.A. Price, Large-scale structure of the Carina nebula. *ApJ*. **532**, L145–L148 (2000)
62. N. Smith, K. Davidson, T.R. Gull, K. Ishibashi, D.J. Hillier, Latitude-dependent effects in the stellar wind of η Carinae. *ApJ*. **586**, 432–450 (2003a)
63. N. Smith, J. Bally, J.A. Morse, Numerous proplyd candidates in the harsh environment of the Carina nebula. *ApJ*. **587**, L105–L108 (2003b)
64. N. Smith, J. Bally, K.J. Brooks, HH 666: the axis of evil in the Carina nebula. *AJ*. **127**, 2793–2808 (2004a)
65. N. Smith, R.H. Barbá, N.R. Walborn, Carina’s defiant Finger: HST observations of a photoevaporating globule in NGC 3372. *MNRAS*. **351**, 1457–1470 (2004b)
66. N. Smith, K.G. Stassun, J. Bally, Opening the treasure chest: a newborn star cluster emerges from its dust pillar in Carina. *AJ*. **129**, 888–899 (2005a)
67. N. Smith, J.A. Morse, J. Bally, The [O III] Veil: astropause of η Carinae’s wind? *AJ*. **130**, 1778–1783 (2005b)
68. M. Tapia, M. Roth, R.A. Vázquez, A. Feinstein, Imaging study of NGC 3372, the Carina nebula—I. UBVRIJHK photometry of Tr 14, Tr 15, Tr 16, and Car I. *MNRAS*. **339**, 44–62 (2003)
69. M. Tapia, P. Persi, J. Bohigas, M. Roth, M. Gómez, Imaging study of NGC 3372, the Carina nebula—II. Evidence of activity in the complex Trumpler 14/Car I photodissociation region. *MNRAS*. **367**, 513–526 (2006)
70. G. Taresch, R.P. Kudritzki, M. Hurwitz, S. Bowyer, A.W.A. Pauldrach, J. Puls, K. Butler, D.J. Lennon, S.M. Haser, Quantitative analysis of the FUV, UV, and optical spectrum of the O3 star HD 93129A. *A&A*. **321**, 531–548 (1997)
71. L.K. Townsley, P.S. Broos, E.D. Feigelson, G.P. Garmire, Parsec-scale X-ray flows in high-mass star-forming regions, in *Massive Star Birth: A crossroads of Astrophysics*, ed. by R. Cesaroni, M. Felli, E. Churchwell, M. Walmsley. IAU Symposium, vol. 227 (CUP, Cambridge, 2005), pp. 297–302
72. R.A. Vázquez, G. Baume, A. Feinstein, P. Prado, Investigation on the region of the open cluster Tr 14. *A&AS*. **116**, 75–94 (1996)
73. N.R. Walborn, Some extremely early O stars near eta Carinae. *ApJ*. **167**, L31–L33, (1971)
74. N.R. Walborn, Some characteristics of the Eta Carinae complex. *ApJ*. **179**, 517–525 (1973)
75. N.R. Walborn, Some morphological properties of WN spectra. *ApJ*. **189**, 269–271 (1974)
76. N.R. Walborn, Forbidden Sulfur II structures in the Carina nebula. *ApJ*. **202**, L129–L130 (1975)
77. N.R. Walborn, The stellar content of the Carina nebula. *Rev. Mexicana Astron. Astrof. Ser. Conf.* **2**, 51–55 (1995)
78. N.R. Walborn, The pillars of the second generation, in *Hot Star Workshop III: The Earliest Stages of Massive Star Birth*, ed. by P.A. Crowther. ASP Conference Series, vol. 267 (ASP, San Francisco, 2002), pp. 111–125
79. N.R. Walborn, The earliest O-type stars, in *A Massive Star Odyssey: From Main Sequence to Supernova*, ed. by K.A. van der Hucht, A. Herrero, C. Esteban. IAU Symposium, vol. 212 (ASP, San Francisco, 2003), pp. 13–21
80. N.R. Walborn, Optically observable zero-age main-sequence O stars, in *Massive Stars: From Pop III and GRBs to the Milky Way*, ed. by M. Livio, E. Villaver. STScI Symposium Series, vol. 20 (CUP, Cambridge, 2009), pp. 167–177
81. N.R. Walborn, E.L. Fitzpatrick, The OB Zoo: a digital atlas of peculiar spectra. *PASP*. **112**, 50–64 (2000)
82. N.R. Walborn, M.H. Liller, The earliest spectroscopic observations of Eta Carinae and its interaction with the Carina nebula. *ApJ*. **211**, 181–183 (1977)
83. N.R. Walborn, et al., A new spectral classification system for the earliest O stars: definition of Type O2. *AJ*. **123**, 2754–2771 (2002a)

84. N.R. Walborn, A.C. Danks, G. Vieira, W.B. Landsman, Space telescope imaging spectrograph observations of high-velocity interstellar absorption-line profiles in the Carina nebula. *ApJS*. **140**, 407–456 (2002b)
85. N.R. Walborn, N. Smith, I.D. Howarth, G. Vieira Kober, T.R. Gull, J.A. Morse, Interstellar absorption-line evidence for high-velocity expanding structures in the Carina nebula foreground. *PASP*. **119**, 156–169 (2007)
86. J.B.Z. Whiteoak, High-resolution images of the dust and ionized gas distributions in the Carina Nebula. *ApJ*. **429**, 225–232 (1994)
87. Y. Yonekura, S. Asayama, K. Kimura, H. Ogawa, Y. Kanai, N. Yamaguchi, P.J. Barnes, Y. Fukui, High-mass cloud cores in the η Carinae giant molecular cloud. *ApJ*. **634**, 476–494 (2005)
88. X. Zhang, Y. Lee, A. Bolatto, A.A. Stark, CO ($J = 4-3$) and [C I] observations of the Carina molecular cloud complex. *ApJ*. **553**, 274–287 (2001)

Eta Carinae and the Supernova Impostors

Davidson, K.; Humphreys, R.M. (Eds.)

2012, X, 330 p., Hardcover

ISBN: 978-1-4614-2274-7